MANCHESTER 1824
The University of Manchester

Embedded RFID Ignition and Power Supply System

Third Year Individual Project – Final Report

April 2019

Youpeng Yu

9952864

Supervisor: Dr Rebecca Todd

School of Electrical and Electronic Engineering

Abstract

This project is to enhances safety system of an electric based kart, by adding keyless locking system and brake lights. The keyless locking system is designed from two perspectives, RFID ignition system and self-locking system. On the other hand, CAN BUS communication system is used to enable communication between brake and brake lights. However, both keyless locking system and brake lights are not battery voltage (48V) rated. The voltage conversion system needs to be designed and implemented to provide 5V and 12V to other electronic devices.

This Report analyse the project from three perspectives including, RFID ignition system, power supply system and brake lights. Designing considerations, test results and analysis will be covered comprehensively for each section.

Contents

Total word count: 10512

1. Introduction

1.1. Motivations

Electric vehicles are powered by electric motors rather than conventional internal combustion engines in the modern petrol cars, and the energy supply of motors is electricity coming from rechargeable batteries.

Comparing electric vehicles with petrol vehicles, electric vehicles have the following benefits. Firstly, electric vehicles are eco-friendly. By eco-friendly, it suggests that electric vehicles can improve air quality and reduce climate change. “2017 UK greenhouse gas emissions statistics” published by government of UK suggests transport accounts for 27% of UK’s carbon emissions. [1] on the other hand, pure electric vehicles can significantly reduce greenhouse gas emission from transport because they do not produce any greenhouse gas exhaust emission. Secondly, electric vehicles are less expensive compared to petrol vehicles regarding daily use. Statistics shows fuel cost of diesel car is around four times than the cost of electricity using by pure electric vehicles. [2]

Moreover, electric vehicles are more adaptive to all kinds of essential electricity-based components such as automotive lighting, sirens and smart key system. Speaking of the smart key system, nowadays, big car companies have already implemented it and they see it as a necessity for modern cars. Therefore, the reason behind that is the smart key systems bring users not just improvements regarding accessibility because it is easier to carry with, but also the safety aspect. To illustrate that, locking systems auto-lock the car after a certain period when users left the car unlocked and the car cannot be ignited when smart keys are not around.

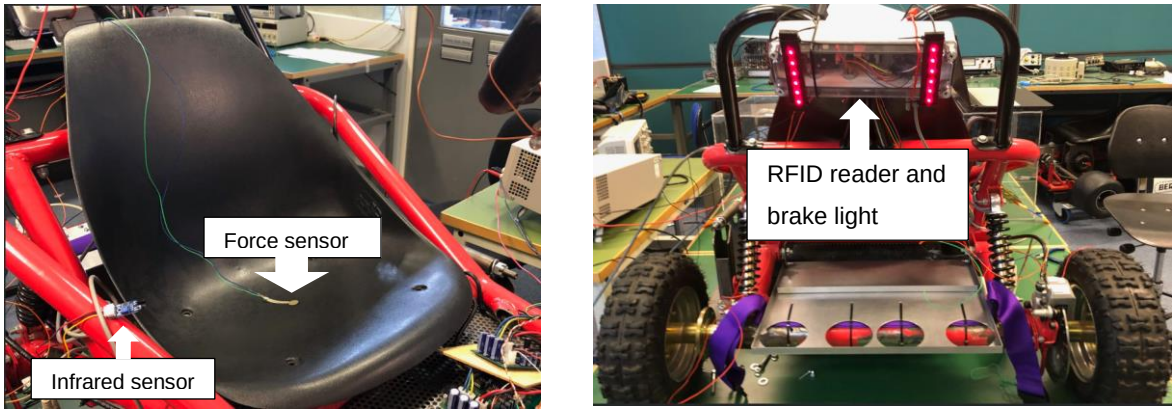

Figure 1. Electrical kart of this project.

Figure 1 shows the working scope of this project, including the sensors, RFID readers and the brake lights. The RFID reader and sensors are used to build RFID ignition system and auto-locking system. The RFID ignition system can enable the kart being used easily by different authorized users by simply adding their RFID tags' UID number into the database of RFID ignition system. Besides, the auto-locking system can ensure the kart is always left in the safe state even when users forgot to lock the kart after using.

Speaking of pedestrian safety, this electric kart does not have a brake light, hence, adding this safety precautions are also part of the project. Nevertheless, most components involved in this project cannot work directly with a 48V supply from battery. As a result, the power distribution problem needs to be solved by building up voltage conversion circuits which can convert 48V into 12V/5V.

1.2. Aims and Objectives

The aim of this project is to enhance owner and pedestrian safety system by adding keyless locking system and brake lights. Moreover, designing PCB circuits capable of converting 48V down to provide 5V for micro-controllers and 12V for brake lights.

This project has the following objectives,

- Design the RFID ignition system.
- Design a self-locking system.
- Provide a 5V and 12V supply.
- Implement the brake lights.
- Enclosure the design.

1.3. Literature Reviews

Nowadays, there are three common key systems of cars, namely, mechanical key-lock systems, remote keys systems and keyless entry-systems. RFID has long been a critical technique to the smart key system because it guarantees safety with a unique encryption technique is applied. RFID is a radio-frequency identification technology which keeps sending radio waves to identify and track tags. RFID has a wide range of applications. For example, RFID applications in healthcare to track medical equipment and patients' files, RFID applications in supermarket to manage stock.

As mentioned above, the smart key system has been widely implemented on board and is considered as necessity for big car companies. For example, BMW has a long history of developing

the smart key system. Nowadays, they even add a display screen on the key fob to display all essential information, such as the status of air condoning, windows, doors and fuel levels. "*The key fob with display is therefore capable of showing the sort of status information that can be accessed on a smartphone with the BMW i Remote app. However, the data is transmitted to this premium key fob by means of the same radio signal used to lock or unlock the vehicle. The information can be updated if the vehicle is within radio range of the key.*" [3]. This short report was published by BMW blog in 2015, and up until that time, RFID was still the most fundamental technology in their smart key systems. However, there will be a step from the smart key towards "keyless" in the future. This "Automotive Application of Biometric Systems and Fingerprint" paper suggests the biometric identification would be the innovation technology to be implemented on cars, and this biometric lock can reduce the risks of theft or loss of property due to driver's negligence.[4] Drivers will no longer have to bring key fobs with them, and biometric locks provides even more safety and convenience by checking fingerprints, iris (a thin, circular structure in the eye) or other biological evidence.

1.4. Structures

In this report, experimental test on RFID ignition system will be discussed in Chapter 2, power supply circuit design will be discussed in Chapter 3, brake lights and enclosure design will be presented in Chapter 4, and lastly conclusion is in Chapter 5.

2. RFID Ignition System

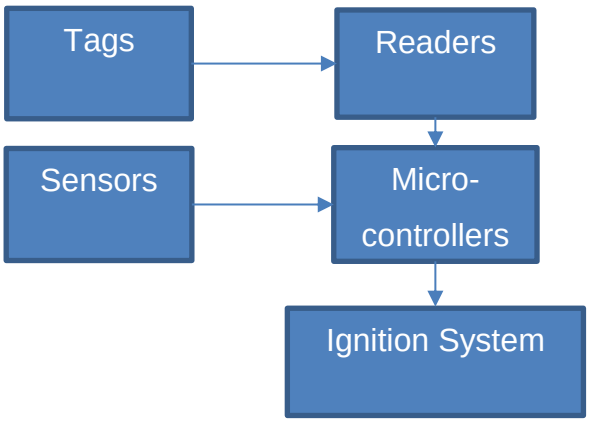

Figure 2. Overview of the ignition system and sensor inputs.

The RFID ignition system is shown in Figure 2, and this diagram is made of 5 main blocks, namely, tags, readers, sensors, micro-controllers and the ignition system.

2.1. Tags

The Tag acts as a key to the RFID ignition system. In other words, the kart can only be ignited when the RFID reader detects the correct UID (unique identification).

2.1.1. Comparisons between tags and selection

	Passive Tag	Active Tag	Semi-passive/active ag
Tag power	Energy transferred from reader	Internal battery	Internal battery/ energy transferred from reader
Working range	Short (up to 10m)	Long (100m or more)	Moderate (Up to 100m)
Price	Cheap (£0.1 or more)	Expensive (£15 or more)	Moderate (£8 or more)
Tag size	Small (25 x 30 x 5 mm)	Big (120 x 36 x 30 mm)	Moderate (130.4 x 23.4 x 12.7 mm)

Table 1. Comparisons between different types of tags.

Table 1 shows general features of all three different types of tags from both physical and commercial aspects, including power source, working range and size and price. Comparing between all three types, passive tags have the following advantages and limitations. Firstly, passive tags are cheap. A typical passive tag is made up of three parts, an antenna, a micro-chip and a substrate which allow components to be mounted on. A typical price of a passive tag is about £0.1 or more. Secondly, passive tags are small. The simple structure of passive tags also suggests the physical size of a passive tag can be extremely small, about 25 x 30 x 5 in mm. Lastly, passive tags are safer in terms of data protection compared with other types of tags. A major concern of RFID tags today is security and privacy problem. To be specific, RFID tags send signals to readers without alerting their owners, therefore anyone can access to this fixed serial number signal within reading range [5]. However, there are still some limitations of passive tags. The lack of on-board power supply affects passive tags' reading range and limits it up 10m. After taking the above aspects into consideration, passive tags are chosen for this RFID ignition system.

2.1.2. Tags implementation

Passive Tags can be further differentiated into LF (low frequency), HF (high frequency) and UHF (ultra-high frequency) by their working frequency range.

	Low Frequency RFID Passive Tag	High Frequency RFID Passive Tag	Ultra-High Frequency RFID Passive Tag
Frequency range	125 kHz and 134.3 kHz	13.56 MHz	860 ~ 960 MHz
Reading range	Read distance of 30 cm (1 foot) or less	Maximum read distance of 1.5 meters (4 foot 11 inches)	Minimum read distance of over 1 meter

Table 2. Comparisons between different frequencies-based RFID tags.

Table 2 shows a positive relationship between working frequency and reading range. In other words, reading ranges extend as working frequency increases. LF and HF RFID passive tags are rather cheap and can easily be bought from online store, such as Amazon. In this case, designing and manufacturing one is not prioritized because that would be time-consuming and less efficient. After exploring the online store, MIFARE® 13.56MHZ TAGS have become the first option at the beginning of this project for several reasons as mentioned below.

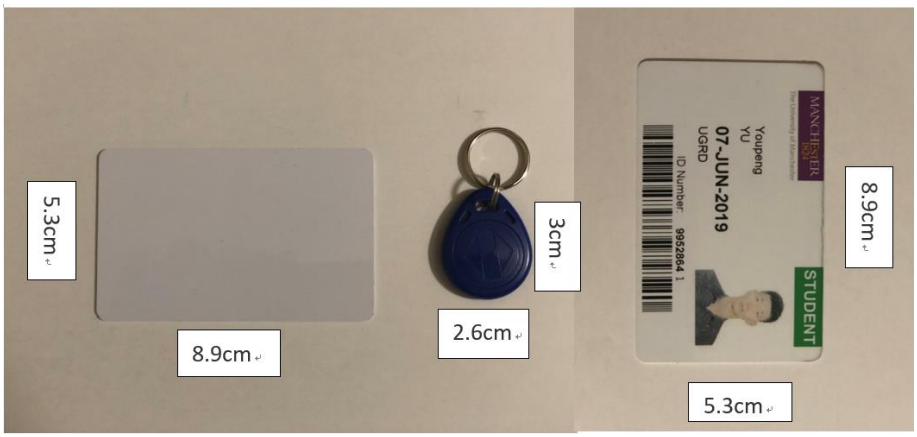

Figure 3. Card type (left) and Key fob (middle) Type Passive Tag & student card (right).

Firstly, MIFARE tags come in many different types of design. Figure 3 shows card type and key fob type of the MIFARE tags. The card type tag has a dimension of 5.3cm x 8.9cm with a rather thin layer that can easily be fitted into a wallet or a card case. The key fob tag has a dimension of 3cm x 2.6cm in plain view with a key ring on the top which can easily be chained to other key rings. Secondly, MIFARE 13.56MHz can be rewritten and duplicated easily using Arduino RFID sensor MFRC522 which is a RFID reader compatible with Arduino microcontroller operating at 13.65MHz.

However, MIFARE tags have been replaced by student cards of Manchester university as the project went along. The student card is also 13.56MHz passive RFID tag, and for a better reason, students in this university must carry their student cards with them all the time. As a result, choosing the student card to be the tag will not create any extra burden to the users, especially when users are

university staff or students.

2.2. RFID Readers and Micro-controllers

Micro-controllers and RFID readers both play important roles in the RFID ignition system. RFID readers are used to detect RFID tags and transmit signals to micro-controllers, then micro-controllers identify the signal received and perform a series of tasks.

2.2.1. Comparisons between RFID readers and selection

RFID readers are used to build up connections between tags and the ignition system. In other words, the correct RFID tag cannot start the kart without the presence of a RFID reader. Most RFID readers are made up of integrated circuits to modulate and demodulate radio frequency signals and then transmit the signal through the antenna of RFID readers.

	Low Frequency RFID Reader	High Frequency RFID Reader	Ultra-High Frequency RFID Reader
Band Frequency	120–150 kHz (LF)	13.56 MHz (HF)	433 MHz (UHF)
Working range	10 cm	10 cm–1 m	1–100 m
Data Speed	Low	Low to moderate	Moderate

Table 3. comparisons between different frequencies-based RFID reader.

RFID readers can be differentiated into three types in common based on their band frequencies, as mentioned earlier, LF RFID readers, HF RFID readers and UHF RFID readers, summarised in Table 3. Band frequency-based RFID readers share some similar properties of RFID tags. As the band frequency increases, the working range and data transferring speed also increases. For example, HF RFID readers have 10cm-1m working range which is larger than 10cm working range of LF RFID readers, but smaller than UHF RFID readers' working range 1-100m.

The main reason of HF RFID readers is chosen for this project is because RFID readers must operate at a band frequency which matches RFID tags' to be able to transmit and receive signals. Therefore, a 13.56 MHz operated passive RFID student card can only be detected by a 13.56 MHz HF RFID reader.

2.2.2. RFID readers implementation

As mentioned before, RFID readers are made up of integrated circuits containing antennas.

Designing and building ICs for RFID readers is not a wise approach for this RFID ignition project since RFID readers satisfy the requirements in Section 2.2.1 can be easily bought from online stores. Furthermore, two HF RFID readers (RS232-B1 v2 and MFRC522) with different features are considered at the start up stage of this project, and they are compared in Table 4.

	RS232-B1 v2 RFID Reader	MFRC522 RFID Reader
Operating Frequency	13.56MHz	13.56MHz
Read range	5cm	3cm
Length x Width	75 x 50 x 3 mm	60 × 39 x 3 mm
Price	£18.11	£5.76
Input voltage	4.5V to 25V	2.5V to 3.3V

Table 4. Comparisons between RS232-B1 v2 and MFRC522.

Information (operating frequency, read range, size, price and input voltage) of two different HF RFID readers are shown in Table 4. The reason to choose two high frequency (13.56MHz) operated RFID readers is both RFID readers are compatible with university student cards, and that gives this ignition system some advantage in tags choosing.

In comparison, MFRC522 readers are cheaper and smaller. RS232-B1 v2 readers (£18.11) are much more expensive than MFRC522 readers (£5.76) because B1 readers provide extra functions beyond the requirements of this ignition system. For example, the B1 reader have voltage regulator on board and this voltage regulator allows the reader to be powered up by an input voltage between 4.5V and 25V. The B1 readers can simply be powered by micro-controller's 5V output, and this wide range of input voltage is not essential for a RFID reader. Furthermore, B1 readers are 15mm and 11mm longer in length and width respectively. The difference in size between two readers suggests that MFRC522 readers take less space.

On the other hand, B1 readers are 2cm longer than MFRC522 readers in terms of reading range. However, both readers' reading ranges are less than 10cm and the this suggests that both readers are NFC readers. NFC stands for near-field communication, and NFC technology is a more finely-honed version of RFID. NFC operates at 13.56MHz as HF RFID does, but it is more secure in terms of data exchange and the maximum reading range is limited (up to 10cm). The advantage of NFC readers for this RFID ignition system is that RFID tags can be prevented from being accidentally detected from a long distance and therefore leads to unwanted tasks being processed. Besides, both RFID readers can be powered by micro-controller using 3.3V and 5V, respectively. To consider the

above analyses of both readers, MFRC522 RFID readers are chosen for this project because RS232-B1 v2 RFID readers cost more money than MFRC522 RFID readers and the additional functions are inessential.

2.2.3. Comparisons between Micro-controllers and selection

Micro-controllers are small computers built on integrated circuits, and are coded to perform a series of tasks by observing the states of digital inputs, analogue inputs and other types of inputs. There are three types of microcontrollers or microchips being considered to optimize the selection of micro-controllers, which are Arduino Uno, Arduino Leonardo CAN BUS shield and ATtiny 45.

	Digital pins	Analogue pins	ICSP pins
Requirements	6 pins	1 pin	6-pin set

Table 5. Requirements on pins of micro-controllers.

	Arduino Uno	Arduino Leonardo CAN BUS shield	ATtiny45
Programming language	Arduino	Arduino	Arduino
Price	£19	£24	£2.1
MCU	ATmega328P	ATmega32U4	ATmega328P
CAN BUS	Extra CAN BUS shield	YES	NO
Digital pins	14	9	2
Analogue pins	6	3	3
ICSP pins	6	6	0
Clock speed	16MHz	16MHz	10MHz
Input voltage	7V-12V	5V-16V	2.7V-5.5V

Table 6. Comparison between different micro-controllers.

Table 5 shows the required number of pins for digital, analogue and ICSP pins. This project requires 6 digital pins. To be specific, it requires 2 digital output pins for LED presentation, 1 digital input pin for the RFID reader, 2 digital input pins for two infrared sensors and 1 digital output pin for the bipolar junction transistor (BJT). Furthermore, 1 input analogue pin is needed for force sensitive resistor. Lastly, 6-pin set ICSP are needed for RFID readers implementation including MISO, MOSI, SCK, RST, 3.3V and GND. After comparing properties shown in Table 6, Arduino Leonardo CAN BUS shield is a better option for the following reasons.

To begin with, this RFID ignition project requires 6 digital pins, 1 analogue pin and 6-pin set ICSP. Arduino Uno can provide 14 digital pins, 6 pins and 6-pin set ICSP and the provided pin numbers of Uno is more than enough. On the other hand, Leonardo CAN BUS shield can provide 9 digital pins, 3 analogue pins and 6-pin set ICSP, and the pin setting of Leonardo is just enough compared with the requirements. To shrink this RFID ignition system, ATtiny45 microchip is also considered at the start of this project, but it is soon excluded from the options because the limitation of digital pins (2 digital pins) and ICSP pins (no ICSP pins set).

Furthermore, Leonardo CAN BUS shield is a shielded Leonardo board which supports CAN bus connection. This connection is rather essential in this project because the brake light needs to be light on whenever the brake of the kart is pressed. This brake signal is monitored by another micro-controller at the front of the kart. Hence, it requires a 9-pin D-SUB cable to transfer the signal from the front to the back of the kart, and a 9-pin D-sub has pin2 represents CAN_L signal and pin7 represents CAN_H signal. Among these three choices, Leonardo CAN BUS shield is the best choice because Arduino Uno board needs an extra CAN BUS shield to be applicable to CAN BUS connection and ATtiny45 cannot work with CAN BUS. This Arduino Uno CAN BUS shield adds extra £25 on the original price making the total price £44 which is rather expensive compared with the price of Leonardo CAN BUS shield (£24).

2.2.4. Connections between RFID readers and Micro-controllers

Since the choice of RFID readers and micro-controllers are chosen to be MFRC522 and Leonardo CAN BUS shield, the connections between them must be made to allow signals to travel through wires from MFRC522 to Leonardo board.

	MFRC522 Reader Pin	Arduino Leonardo CAN BUS shield
RST/Reset	RST	ICSP-5
SPI SS	SDA(SS)	Pin 10
SPI MOSI	MOSI	ICSP-4
SPI MISO	MISO	ICSP-1
SPI SCK	SCK	ICSP-3
Power	3.3V	ICSP-2
GND	GND	ICSP-6

Table 7. Pin layout of MFRC522 reader and Leonardo CAN BUS shield

As can be seen from Table 7, 5 different types of signals besides the power and ground need to be

transferred from reader to the micro-controller. These signals are RST (reset), SPI SS (serial clock), SPI MOSI (Master Output Slave Input), SPI MISO (Master Input Slave Output), SPI SCK (serial clock).

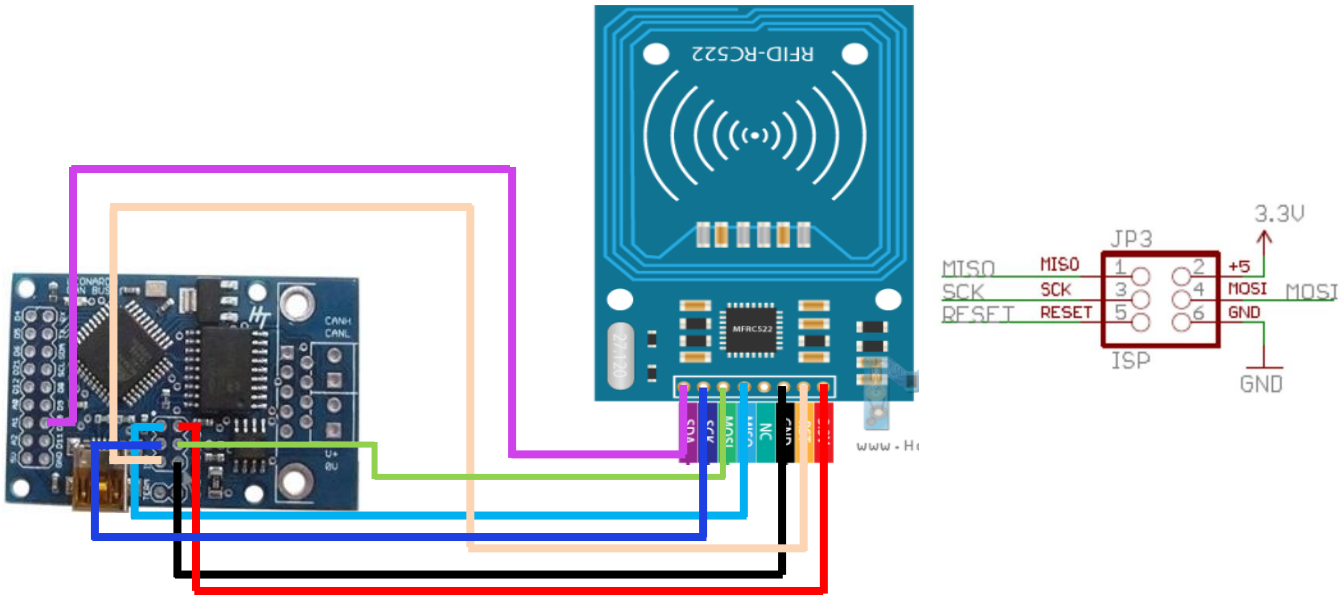

Figure 4. Connections between MFRC522 and Leonardo CAN BUS shield and 6-pin ICSP set.

Figure 4 shows the wiring diagram between MFRC522 and Leonardo CAN BUS shield and the pin layout of the ICSP port. To be specific, the ICSP port are connected to the matching signal output of the MFRC522 readers, and the SDA(SS) pin on the MFRC522 is connected to pin D10 by default setting in the Arduino library.

2.3. Sensors

In this RFID ignition system, a self-locking system is designed for security consideration. To be specific, the kart can be locked automatically after a period of time provided no one is on the kart. In the meantime, the measurements of “if someone on the kart” have to be conducted by sensors which can precisely reflect the seating status of the kart.

Two types of sensors, infrared sensors and force sensitive resistors, are considered as user-detection sensors at the beginning of this project. However, these sensors behave differently, and it is hard to choose which one fits more without testing them. For testing purposes, FC-51 IR proximity sensors are chosen as infrared sensor and FSR406 (38 x 38mm) Square Force Sensing Resistor is chosen as force sensors.

2.3.1. Force sensitive resistor

Force sensitive resistors (FSR) are resistors but with resistance change accordingly to force. Since FSRs are the fundamental components which can hardly be designed and built in this project, the best option is to purchase from online stores. In this case, the biggest size of FSR can be bought from Rapid is 38 x 38mm.

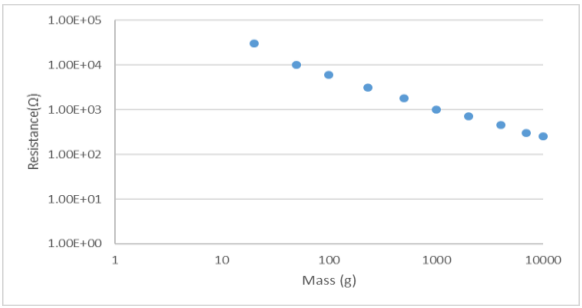

Figure 5. The logarithmic scale plot of resistance against mass.

Figure 5 is a logarithmic plot of resistance in ohms against mass in grams and redrawn from datasheet [6], the table of data points used in the graph plotting are in Appendix 5. There is a rough linear relationship between resistance and mass provided both in logarithmic scale. In other words, resistance changes dramatically at low mass end of the mass-resistance characteristic, but only changes slightly at the high mass end. For example, resistance of FSR drops 20k when the mass on the pad is increased from 20g to 50g, but only drops 50ohms when mass on the pad increases from 7kg to 10kg.

2.3.2. Force sensitive resistor implementation

From figure 6, the basic hardware implementation of FSR is building a 5V voltage divider together with a 1k-ohm resistor and measuring the voltage across the 1k-ohm resistor with analogue input pin A0 from the Leonardo CAN BUS shield.

For the software implementation, 500 is selected in the Arduino code to be the boundary value for easier calculation because 500 is about the median compared to the input range of pin A0 (0 to 1023). To elaborate on that, the input value of A0 can be calculated from equation (1) by replacing the value of resistance of FSR.

$$A0 = \frac{1000}{1000+R_{FSR}} \times 1023 \quad (1)$$

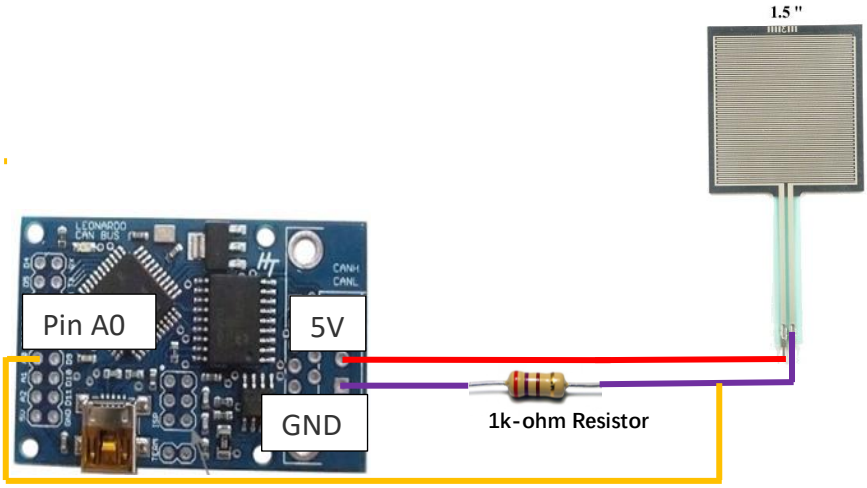

Figure 6. Connections between FSR and Leonardo CAN BUS shield

In Section 2.3.5, the Arduino code of sensor implementation is given as,

```
if (force < 500) {digitalWrite(LED_G, LOW)};
```

This line of code says that when the pin A0 has a reading smaller than 500, then no one is detected on the kart through FSR and turns off the green LED. In this case, the green LED is turned off to indicate power supply of the kart is cut off. Furthermore, the voltage across the 1k-ohm resistor is below 2.5V when reading of pin A0 is smaller than 500. In other words, FSR takes over half of the voltage supply when FSR's resistance is bigger than 1k-ohm resistor. In Appendix 5 "mass-resistance characterises of FSR", FSR only has a resistance higher than 1k ohms when the mass on the pad of FSR is bigger than 1kg.

The resistance of fixed value resistor in series of FSR cannot be too high; hence, the kart cannot automatically lock itself. On the other hand, the resistance of the fixed value resistor cannot be too small, hence, the kart shuts the power supply even with people are driving the kart. As a result, 1k-ohm resistor is chosen carefully, and the kart still can lock itself with mass on the kart smaller than 1kg.

2.3.3. Infrared sensor

Infrared sensors are rather complicated and delicate devices which contain Infrared emitters, infrared receivers, potential meters, comparators and other components. E18-D80NK and FC-51 are both IR sensors which satisfy the requirements of user detection sensors. Since these two sensors can both be bought from online stores for a rather cheap price, then it was not necessary to design

and build one for this RFID ignition system.

	E18-D80NK IR sensors	FC-51 IR proximity sensors
Shape	Cylinder	Cuboid
Size	Length x Width: 45 x 17 mm Diameter:18mm	Length x Width: 45 x 14 mm Thickness:7mm
Supply voltage	3.3V- 5V	5V
Detection angle	35 degrees	<15 degrees
Detection distance	3-80 cm	2-30 cm
Price	1 piece for £6.99	5 pieces for £8.89

Table 8. Comparisons between E18-D80NK IR sensors and FC-51 IR proximity sensors.

From table 8, there are three key difference between E18-D80NK sensors and FC-51 sensors, which are detection parameters, shape of sensors and prices. Firstly, detection parameters, detection distance and detection angle, of two sensors are rather different. E18-D80NK sensors' detection distance (3-80 cm) is much longer compared with FC-51 sensors' (2-30 cm), and the detection distance of both IR sensors can be adjusted by potential meters on board. However, the required detection distance under normal conditions are only about 20cm. Thus, both IR sensors satisfy this detection distance requirements. From detection angle perspective, FC-51 sensors have extra 20 degrees of detection range than E18-D80NK sensors, which is the main reason for choosing FC-51 as IR sensors. To be specific, FC-51 sensors can still detect users when they are leaning forward or backword with extra detection angle. Secondly, the shape of two sensors are different. E18-D80NK sensors are cylinders with diameter of 18mm, and FC-51 sensors are cuboid with thickness of 7mm. Since the length and width of two sensors are similar, thin layer-built FC-51 is more easily to be fixed on the handle of kart. Lastly, prices of two different sensors are rather different. E18-D80NK have a unit price of £6.99, but FC-51 only costs less than £2 for each unit. On top of that, FC-51 sensors have larger range of input voltage from 3.3V-5V compared with E18-D80NK's 5V input voltage. After taking the above comparisons into considerations, FC-51 IR proximity sensors are chosen to do some tests as IR sensors.

2.3.4. Infrared sensor implementations

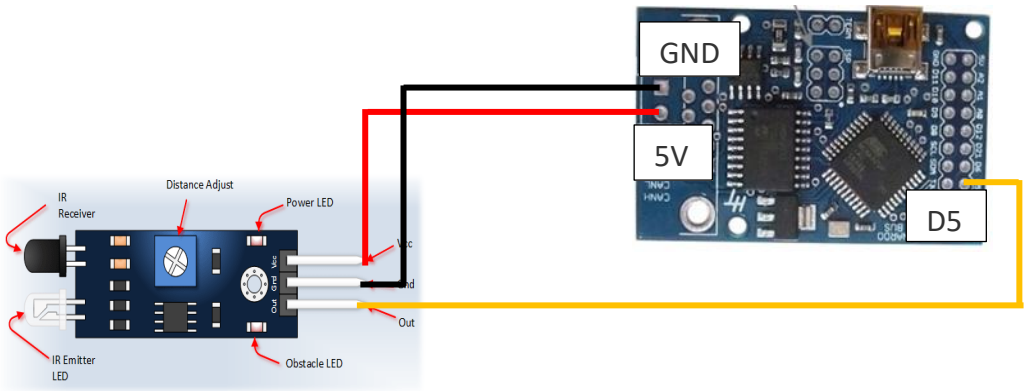

Figure 7. Connections between Infrared sensor and Leonardo CAN BUS shield.

For the hardware implementation, FC-51 IR proximity sensors have three pins need to be connected, including pin Vcc, pin GND and pin Out. Specifically, pin Vcc and pin GND are responsible for power supply and pin Out is for signal output. Furthermore, Table in Appendix 6 and Figure 7 show the pin layout and physical connection for FC-51 and Leonardo, respectively.

For the software implementation, pin Out is a digital output pin which means it only outputs a "HIGH" state or a "LOW" state. Hence, a digital pin D5 on Leonardo board is chosen and defined to be digital input. In Section 2.3.5, the Arduino code of sensor implementation is given as

```
if (isObstacle == HIGH) {digitalWrite(LED_G, LOW)};
```

This line of code relates to IR sensors and means when the pin D5 reads a "HIGH" signal, then no one is detected on the kart through IR sensors and turn off green LED. In this case, turn off green LED is a showing of cut off the power supply of the kart.

2.3.5. Sensors comparisons and solution

	Force sensitive resistor	Infrared sensor
Advantages	• Posture irrelevant (provided sit on FSR)	• Users can be detected even stand up a little
Disadvantages	• Detection area limited (38.1mm x 38.1mm) • Users need to sit on FSR to be detected	• Detection angle limited (35 degrees)

Table 9. Comparisons between FSR and IR sensors.

Table 9 shows the advantages and disadvantages of FSR and IR sensors, and this can be utilized to give the final solution of user detection system.

The final solution of user detection system is using two infrared sensors and two FSR. To be specific, two infrared sensors are fixed on the handle besides the driving seat at different angle to detect drivers. This way, users can still be detected when they are leaning forward or backward because of increasing detection angle.

Furthermore, two FSR are fixed at front and at back of the seat respectively. The detection area is limited to 38.1mm x 38.1mm for one FSR but increasing the number of FSR can effectively increase the sensing area of the seat. Which gives user more freedom in sitting posture because they do not have to sit on a specific spot to be detected.

The combination of FSR and infrared sensors give this user detection system more information regarding seat status. To elaborate on that, users may not be detected by FSR when they stand up, but they will still be detected by infrared sensors. The final solution of user detection system is to make sure users are always detected by one of sensors no matter what kind of sitting posture they are using.

However, there is a limitation on the existing final solution of user detection system. To be specific, FSR will trigger the user detection system when small but heavy object left on the seat. Furthermore, the kart will not be able to self-lock with this small heavy object on the seat and this may lead to potential theft.

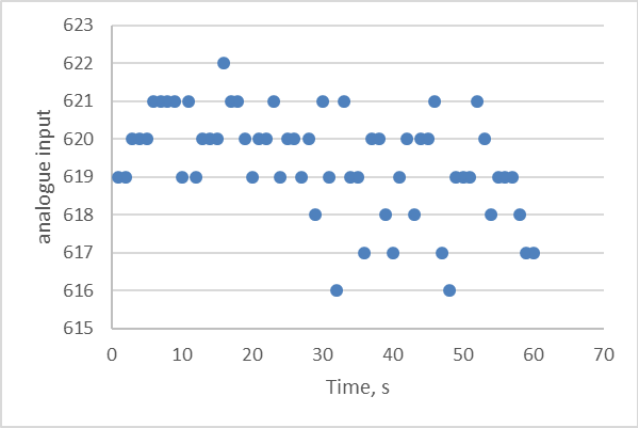

Figure 8. FSR analogue output with user sit still

Figure 8 is the test result of FSR output when user is trying to sit still. It can be seen from figure 8 that there is still some small variation range in the analogue output value from FSR. This means the user detection system can track the output value from FSR in 5 seconds and see if there are any changes. On the other hand, FSR would have constant output value when it detects an heavy object.

In the meantime, the user detection system can recognize that the detection from FSR is an object but not the driver. Therefore, the kart will still be self-locked even with heavy object placed on the seat.

2.4. Coding and logics of locking system

The RFID ignition system of this project can be split into two different parts, namely, self-locking system and RFID tag locking system, as described by flowchart in Figure 9. Furthermore, this code is written using Arduino language because the micro-controller is an Arduino board.

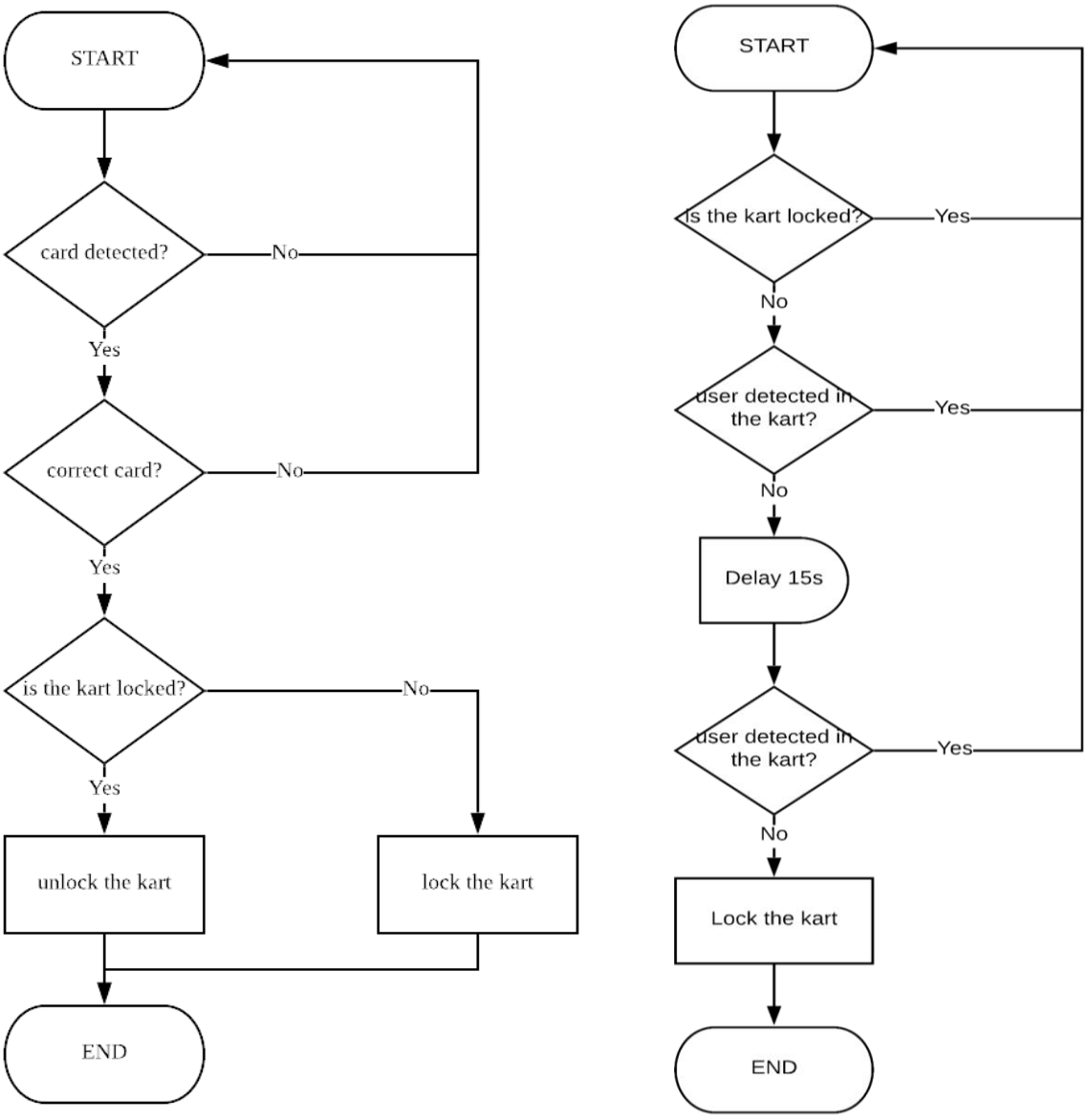

Figure 9. Flowchart of RFID tag locking system (left) and self-locking system (right).

There are a few things that are not shown explicitly from programming perspective in Figure 9.

- Any cards detected?

- Is the card correct?
- Is the kart locked?
- Unlock/Lock the kart.
- Any users detected in the kart.

2.4.1. "Any cards detected?" implementation

This RFID ignition system identifies whether RFID tags are detected by calling a Boolean type function named "`virtual bool PICC_IsNewCardPresent();`" in *MFRC522.h* library. The Arduino code of this function is in Appendix 1.

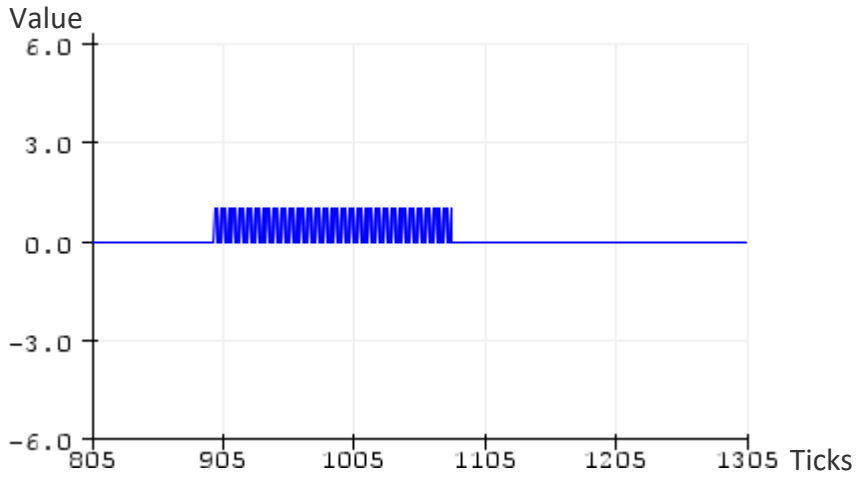

Figure 10. Serial plotter graph of "`rfid.PICC_IsNewCardPresent()`" function.

Since the type of this function is Boolean, the return value of this function either 1 or 0. To elaborate on that, the return value of 1 means true condition and there is a card detected. On the other hand, 0 means no card is detected.

The RFID tag is placed in front of the RFID reader for a while, and Arduino serial plotter is used to capture the waveform of the return value. To do that, only a single line of code in the main loop is needed "`Serial.println(rfid.PICC_IsNewCardPresent());`". Figure 10 shows the return value of this function becomes constantly changing value between 1 and 0 instead of a constant value of 1 for a period of time because this function resets after it is executed.

2.4.2. "Is the card correct?" implementation

This RFID ignition system determines whether the new card is the correct one by calling a Boolean type function "`IsNewCardCorrect()`". The code of this function can be found in Appendix 2.

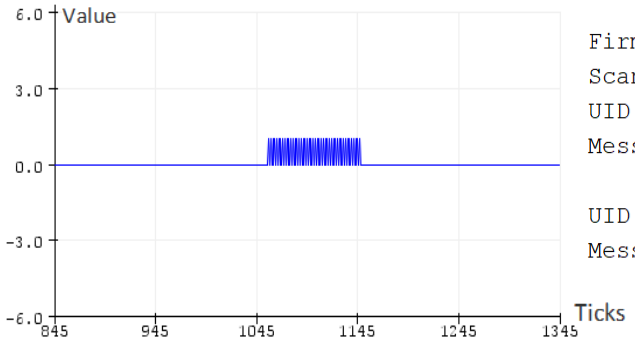


```
Firmware Version: 0x12 = counterfeit chip
Scan PICC to see UID, SAK, type, and data blocks...
UID tag : 04 5D 53 6A 5E 43 80
Message : Authorized Acess

UID tag : CD D9 4A 73
Message : No Acess
```

Figure 11. Serial plotter graph (left) and serial monitor (right) of "`IsNewCardCorrect()`" function.

This function is also a Boolean type and have 1 or 0 as return value. In this case, "1" represents the card detected have access to the kart. On the other hand, "0" represents either no card is detected, or the card detected does not have access to the kart. This function cannot be presented independently because the RFID reader can only identify the card's UID by using the previous function "`rfid.PICC_IsNewCardPresent()`". Furthermore, if no card is detected, this Boolean function will return a 0 because it should return the previous Boolean function's return value which is 0.

"`if (content.substring(1) == "04 5D 53 6A 5E 43 80")`", this "if" statement then decides whether the new card detected is correct or not. On the left side of this if statement, the hexadecimal UID number of the new card detected is recorded in a string type variable named "content". On the right side, the predefined hexadecimal UID number is "04 5D 53 6A 5E 43 80".

From Figure 11 (left), serial plotter graph shows a constantly changing value between 1 and 0 when the correct card is detected in front of the RFID reader because this function resets once it is executed. When the wrong RFID card or no RFID card is detected, this graph shows a constant 0. From the serial monitor in Figure 11 (right), the first card detected has the matching UID number and a message "authorized access" is printed out. On the other hand, the second card does not match the UID number in the database, and hence a message "no access" is printed out.

2.4.3. "Is the kart locked?" and "unlock/lock the kart" implementation

This RFID ignition system uses an integer variable r to record the locking state of the kart and represents the locking state with a green light for simple illustration. Furthermore, the code of this Section can be found in Appendix 3.

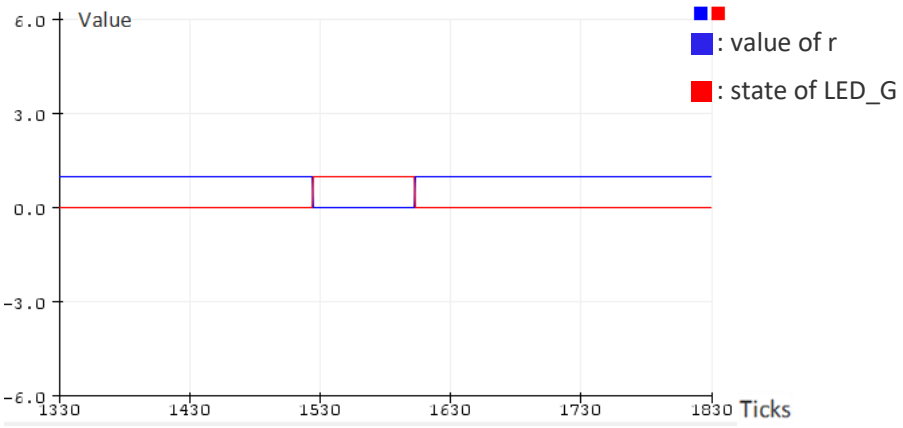

Figure 12. Serial plotter graph of variable r and digital output of LED_G pin.

	Locking state variable "r"	Output state of LED_G pin
The kart is locked	Value of 1 will be stored into r	write LED_G pin with "LOW"
The kart is unlocked	Value of 0 will be stored into r	write LED_G pin with "HIGH"

Table 10. state changing of variable r and LED_G pin.

From Table 10, variable r and LED_G pin have the opposite state value under the same condition. This is set to make sure serial plotter graph in Figure 12 can precisely capture both waveforms without overlapping. Variable r and LED_G pin are initialised to be 1 and LOW, respectively. From Figure 12, the red line (LED_G) is showing 0 and the blue line (r) is showing 1. Both lines are indicating the kart is initialised as locked.

At 1520 ticks, the correct card is displayed in front of the RFID reader to unlock the kart. The red line (LED_G) changes to 1 from 0, and the blue line (r) changes from 1 to 0. The green light is turned on when the correct card is detected. At 1600 ticks, the correct card is tapped again to lock the kart. The red line (LED_G) drops back to 0 and the blue line (r) is also restored as 1. As a result, the green light is turned off indicating the kart is locked again.

2.4.4. "Any users detected in the kart?" implementation

The user detection system is constituted of infrared sensors and force sensors. Infrared sensors and force sensors have digital outputs and analogue outputs, respectively. Figure 13 (left) shows how analogue output from force sensors varies when force is applied on it. At 8225 ticks, the analogue output increases dramatically to about 850 because force is applied on the sensor. Another 60 ticks after, the output drops back to around 30 when the force is no longer exert on. The code for user detection system is in appendix 4.

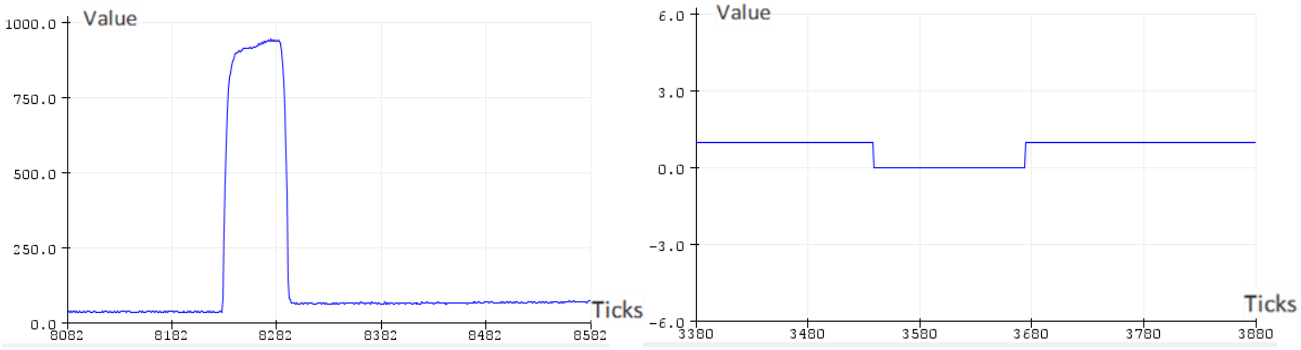

Figure 13. Serial plotter graph of input from force sensor(left) and infrared sensor(right).

On the other hand, Figure 13 (right) shows the variation of digital output from the infrared sensor when an object is detected by the sensor. At 3530 ticks, the digital output from force sensor drops from 1 to 0 because objects are detected. About 140 ticks after, the output value is restored to 1 when nothing is detected by the infrared sensor.

	Infrared sensors	Force sensors
Type of outputs	Digital output	Analogue output
Output value when user detected	0	Depends on the force excreted on; 800 or above (People sitting on)
Output value when no detection	1	20 (no force exerted on)

Table 11. Sensors outputs under different circumstances.

Table 11 summarises the output results observed from Figure 13, and a Boolean type function can be used to determine the user detection result from the two sensors.

```
bool Detection(){
     force = analogRead(pressurePin);
     isObstacle = digitalRead(isObstaclePin);
     if (force > 500 || isObstacle == LOW) return true;
     else return false;
 }
```

The above few lines of codes read sensors, then evaluate readings using an if statement and returns detection results. If there are users detected, then this Boolean type function will return true, else it returns false.

Figure 14 illustrates how self-locking system works based on detection results. It can be seen that the self-locking system does not lock the kart when false detection is only short period, but the locking system does lock the kart when that false detection period is longer than 15s.

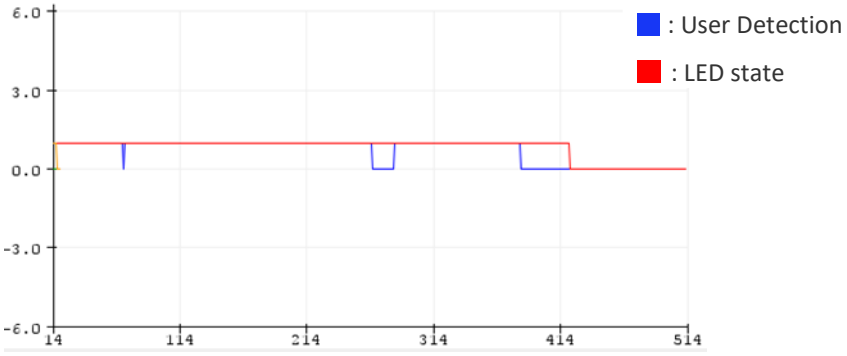

Figure 14. Serial plotter graph of self-locking system.

Lastly, this RFID ignition system described above can perform the following tasks,

- Lock the kart 15s after users' leaving.
- Tap the card to unlock the kart when kart is locked.
- Tap the card to lock the kart when the kart is unlocked.

3. Power Supply System

The battery on the kart can supply is 48V, but microcontrollers and brake lights on the kart need 5V and 12V input voltage, respectively.

3.1. Voltage step-down methods

Two approaches were considered to step down the voltage supply, namely, voltage divider circuit and buck converter circuit. Buck converter circuit is chosen for this voltage step down system because it has significantly higher efficiency than voltage divider circuit.

3.1.1. Voltage divider circuit

Voltage divider is a passive linear circuit which produces an output voltage that is a friction of input voltage. In this case, 48V is the input voltage and 5V is the desired output voltage.

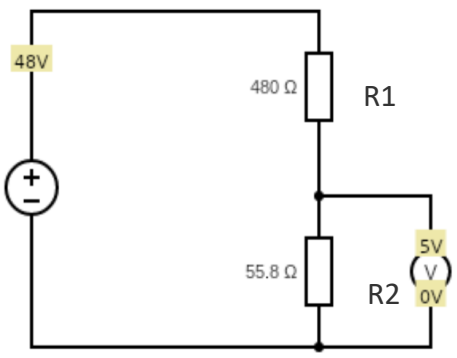

Figure 15. Voltage divider circuit with 48V input and 5V output.

$$Vin = \frac{R1}{R2 + R1} \times Vout \tag{1}$$

Figure 15 shows a voltage divider circuit produces a 5V output across R2 resistor, and the value of resistor of R1 and R2 is determined using equation (1). In this case, R1 is a fixed value resistor of 480Ω and R2(55.8Ω) is the parallel resistance of a fixed value resistor and the microcontroller. However, there are a few limitations of this approach. Firstly, microcontrollers don't have fixed values of resistance which leads to a constantly changing parallel resistance of the microcontroller and the fixed value of resistor. Therefore, the voltage across R2 will no longer be a stable 5V.

$$Efficiency = \frac{P_{OUT}}{P_{IN}} = \frac{V_{out} \times I_{out}}{V_{in} \times I_{in}} \tag{2}$$

Secondly, the efficiency of this voltage divider approach is quite low. Since the resistance of microcontrollers varies in a big range, hence, there will calculate efficiency with 100Ω resistor instead of a microcontroller just to show the poor efficiency of voltage divider method. The input current and output current are calculated using KCL and KVL to be 89.6mA and 50mA, respectively. Therefore, the efficiency of this voltage divider circuit is calculated using equation (2) to be 5.8%.

3.1.2. Buck converter circuit

Buck converter is a great option to step voltage down because no power losses throughout the circuit if neglecting the conduction losses of switches and other passive components.

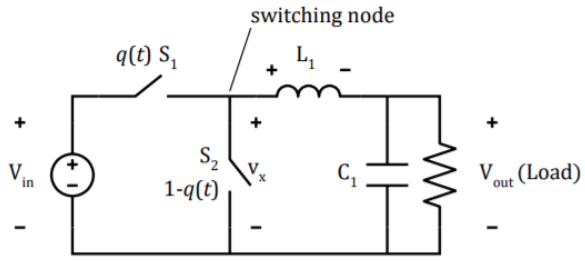

Figure 16. Buck converter circuit [7]

Switch S_1 and S_2 in Figure 16 are complimentary switches, which means S_1 will be on for DT time and S_2 will be on for (1-D)T time. D is the duty ratio, and T is period of switching. In steady state, the voltage across L_1 is zero, therefore $V_x = V_{out}$.

$$V_X = \frac{1}{T} V_{in} DT = V_{in} D \tag{3}$$

$$\frac{V_{out}}{V_{in}} = \mathrm{D} \tag{4}$$

Since S_2 is on for DT period, then the rms voltage across S_2 can be calculated by equation (3). Therefore, the relationship between V_{in} and V_{out} can be rewritten as in equation (4).

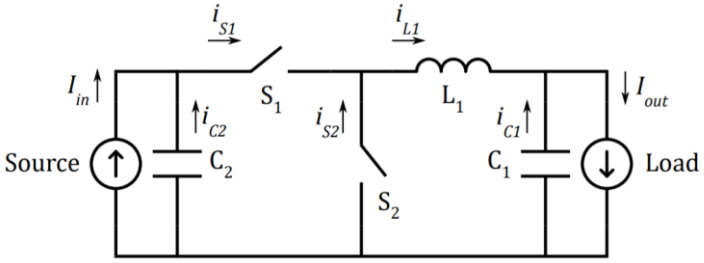

Figure 17. Buck converter with current source and sink [7]

$$I_{in} + i_{S2} = \mathrm{I}_{out} \tag{5}$$

$$i_{s2} = \frac{1}{T} I_{out}(1 - D)T = I_{out}(1 - D) \tag{6}$$

$$I_{in} = DI_{out} \tag{7}$$

Using KCL to analyse the circuit shown in Figure 17, equation (5) can be derived by assuming current going through C_1 and C_2 are zero in the steady state. Furthermore, i_{s2} equals to I_{out} when S_2 is on, which lasts for (1-D)T time. The current through switch 2 can be written as equation (6).

$$I_{in} \times V_{in} = I_{out} \times V_{out} \tag{8}$$

Replacing i_{s2} in equation (5) with i_{s2} expression, the relationship between I_{in} and I_{out} can be written using duty cycle D as in equation (7). Lastly, subsisting duty cycle D in equation (4) with D in equation (7), the equation (8) will be derived showing the constant power of the buck converter.

3.2. Buck Converter Implementation

The buck converter circuit can be built from a LM2574HV DIP-8 (Dual in-line package) IC (integrated chips). This HV version can extend the input voltage range from 4V-40V up to 7V-60V which satisfy the 48V input requirement.

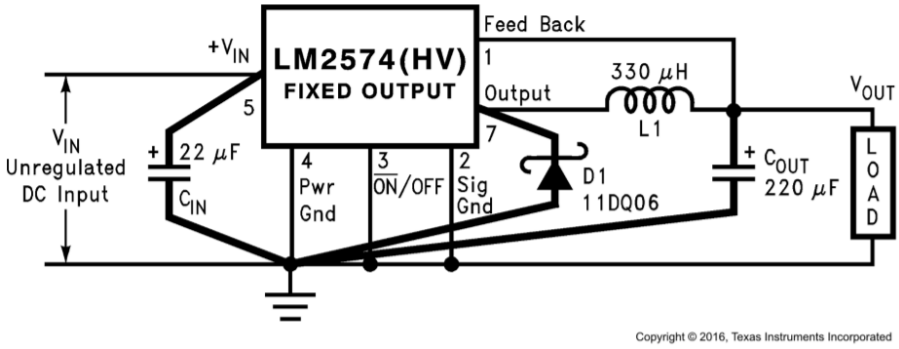

Figure 18. Fixed Output Voltage Version [8]

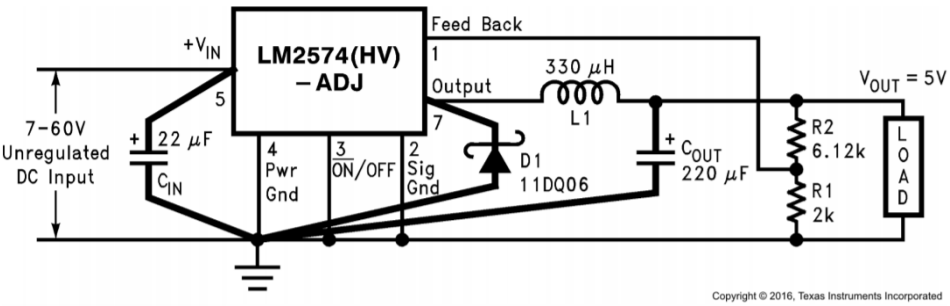

Figure 19. Adjustable Output Voltage Version [8]

Furthermore, LM2574HV can be further differentiated into fixed voltage output version and adjustable voltage version. There are four fixed voltage output versions, including 3.3V, 5V, 12V and 15V. Comparing between Figures 18 and 19, two resistors are omitted in fixed output voltage version because the output voltage of adjustable version is programmed by selecting appropriate resistor values. Since 5V and 12V fixed output version satisfy the requirements and omit two resistors in circuit design, 5V and 12V fixed output version are chosen for buck converter designing.

As can be seen from Figure 18, two capacitors including C_{IN} and C_{OUT}, inductor L1 and Schottky diode D1 are extra components needed to form a buck converter. The requirements of each components for 5V and 12V are summarised in table 12.

	12V fixed output version	5V fixed output version
Capacitor C_{IN}	22-µF, 63V rated	22-µF, 63V rated
Capacitor C_{OUT}	470-µF, 25V rated	470-µF, 10V rated
Schottky Diode D1	0.5-A rating, 63V rated	0.5-A rating, 63V rated
Inductor L1	2200-µH, 0.5A rated	680-µH, 0.5A rated

Table 12. Components selection for 12V and 5V fixed output version.

Capacitor C_{IN} is located between the input voltage 48V and ground 0V to provide enough bypassing for a stable operation of the circuit. Since the input voltage for both 5V and 12V are 48V, then 22µF, 63V rated C_{IN} are chosen for both circuits. 22µF is the system suggested capacitor value and 63V rated is 1.25 times greater than the input voltage for safety consideration.

Capacitor C_{OUT} is placed across the output voltage for stable operation and an acceptable output ripple voltage. The datasheet suggests the capacitance of this C_{OUT} should be a value between 100µF and 470µF. For less ripple consideration, 470µF are picked for both circuits. Furthermore, the voltage rating of the capacitor must be 1.5 times greater than the voltage output. Therefore, 10V rated capacitor is chosen for 5V circuit and 25V rated capacitor is chosen for 12V circuit.

	48V-12V buck converter	48V-5V buck converter
Maximum load current with 20% margin	100mA	300mA
Powered device	Brake light strip (70mA rated)	Leonardo CAN BUS shield (60mA rated) Leonardo (60Ma rated) Uno + Spark fun CAN shield (60 mA rated) Mbed nxp LPC1768 + CAN transceiver nxp 8 pin IC (60 mA rated)

Table 13. Maximum load current and powered device for 12V and 5V buck converter.

The current rating of Schottky diode D1 must be 1.5 times greater than the maximum load current, and the voltage rating must be 1.25 times greater than input voltage. From Table 13, the maximum load current of 12V and 5V circuit are 100mA and 300mA, respectively. Therefore, 0.5A current rated and 63V voltage rated Schottky diode are chosen for 12V and 5V circuit.

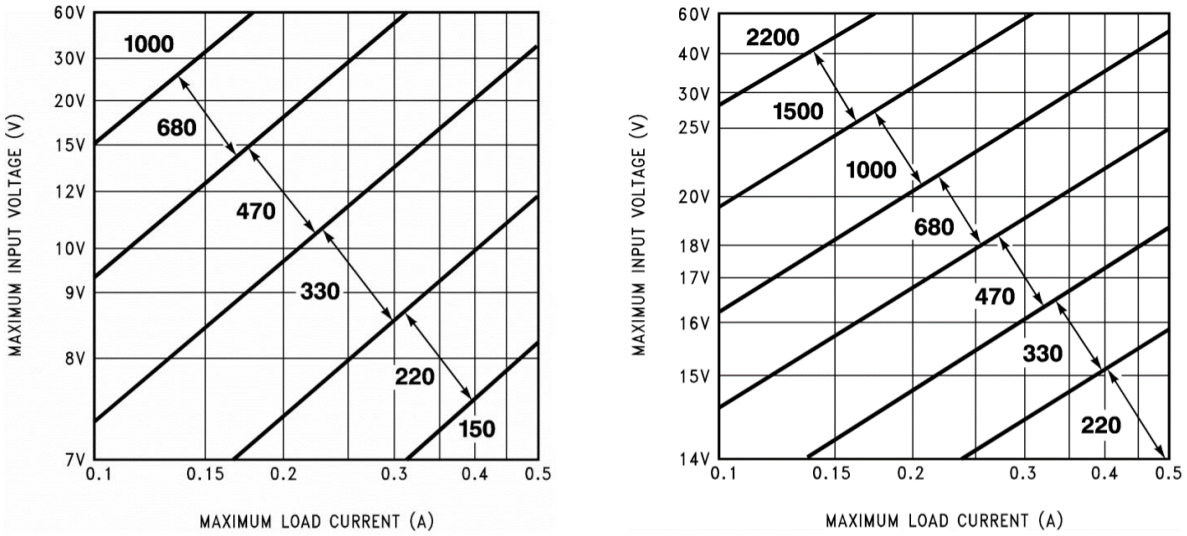

Figure 20. 5-V Inductor Selection Guide (Left) and 12-V Inductor Selection Guide (Right) [8]

Inductance of inductor L1 is chosen based on maximum load current and maximum input voltage. From Table 13, the maximum load current of 12V and 5V are 100mA and 300mA, respectively. Since the input voltage for both circuits are 48V, the inductance area of both circuits can be identified by cross comparing maximum input voltage and maximum load current. By doing this method, inductance of L1 is identified to be 2200µH for 12V circuit from the Figure 20 (right) and inductance of L1 is identified to be 680µH for 5V circuit from the Figure 20 (left). Lastly, the current rating for both inductors are 0.5A because they should be at least 1.25 time greater than the maximum load current.

3.3. PCB Design

Both 5V and 12V buck converter circuits are tested using breadboard and guaranteed to work. PCB is chosen to present the final project rather than stripboard for a few reasons. For example, PCB has much stable connection compared with stripboard. Also, PCB has labels and polarity on components, but not for stripboard design. Last but not least, PCB has lower electronic noise than stripboard design because trail length between component are decreased if properly design.

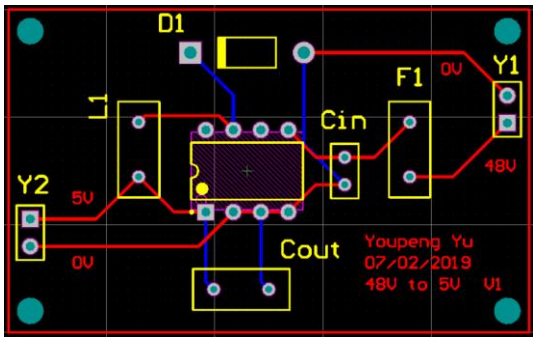

Figure 21. Buck converter PCB design

Figure 21 shows the designing document of buck converter PCB, and there are some good sides of this design. Firstly, all components on the PCB are placed tightly and logically. As a result, trail length between components become quite small. Secondly, two headers are placed at opposite side of PCB. This design gives more natural connections between buck converters and other components. Lastly, terminal voltages and step-down voltage are labelled on board. Since there are two versions including 5V and 12V, labels of step-down voltage become rather important for buck converters to be identified. Moreover, terminal voltage labels can better help designer distinguish the input and output side of the buck converter and avoid reversing polarities.

3.4. PCB Testing

Buck converter PCBs (5V and 12V) are taken to test using digital multimer and oscilloscope. From Figure 22, both 5V and 12V buck converters are powered by DC power supply with 47.98V. To be more specific, this DC power supply machine has two power supply terminals and the right terminal with wires plugged-in is used. Since there are no load on the stepped down side of buck converters, there is 0A current being supplied by the DC power supply.

From Table 14, the percentage difference of 12V version is 0.38% lower than 5V version which means 12V version is compared to be more successful in terms of stepping down 48V input voltage, and this difference may be due to different step-down amplitude. 12V-buck converter is performing better because it only has 36V step-down amplitude, but 5V-buck converter has 43V step-down

amplitude. More experiments can be conducted to prove or disapprove this conjecture.

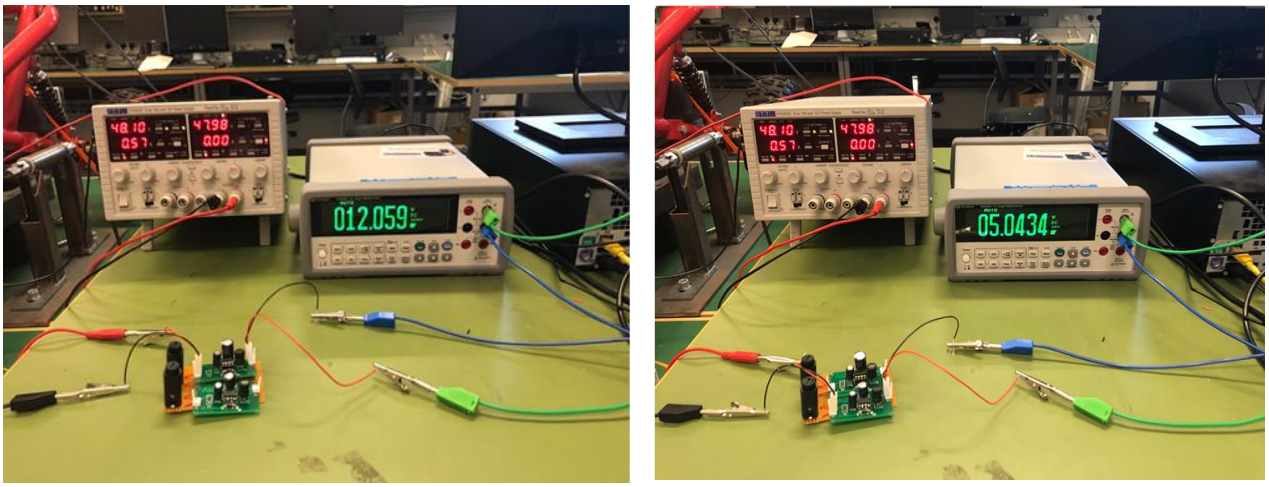

Figure 22. Measurements of 12V(left) and 5V(right)using digital multi-meters.

	5V-buck converter	12V-buck converter
Input voltage	47.98V	47.98V
Current flowing	0A	0A
Output voltage	5.0434V	12.059V
Percentage difference (rated V_{out} and actual V_{out})	0.87%	0.49%

Table 14. 5V and 12V buck converter measurements from DMM.

However, the percentage differences of both buck converters are small and can be used to supply 12V rated brake lights and 5V rated microcontrollers.

Figure 23. Measurements of 12V(left) and 5V(right) using oscilloscopes.

Figure 23 shows voltage waveform of 5V and 12V buck converters. Both waveforms are looking rather straight, which suggests that both buck converters provide constant output voltage.

	5V-buck converter	12V-buck converter
V_{max}	12.0V	5.04V
V_{min}	11.6V	4.08V
V_{pp}	400mV	160mV
V_{avg} or V_{rms}	11.8V	5.00V
Percentage variance (V_{pp} / V_{rms})	3.39%	3.2%

Table 15. 5V and 12V buck converter measurements from oscilloscope

Table 15 presents readings from oscilloscope, which are different from the ones obtained from DMM in Table 14. This is because oscilloscopes are not as accurate as DMM in terms of voltage measurements. The percentage variance of output voltage for both buck converters can be calculated using equation (9). Furthermore, the output voltages of 5V and 12V buck converters have relative low percentage variance, and that further proves the output voltage is constant.

$$\text{Percentage variance} = \frac{V_{peak-peak}}{V_{rms}} \times 100\% \quad (9)$$

4. Brake Lights and Enclosure Design

4.1. Brake Lights

The kart used in this project lacks of brake light which is indeed very important for safety considerations. In this project, the microcontroller used to control RFID ignition system together with bipolar junction transistor are also used to control the brake light on the kart. Figure 24 shows the circuits of brake light controlled by microcontroller.

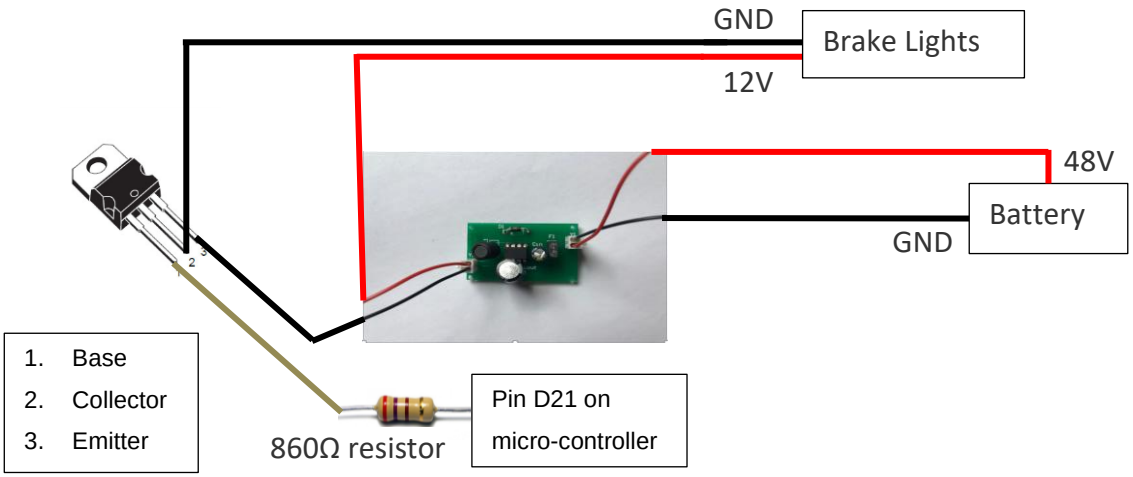

Figure 24. Brake light system.

4.1.1. Bipolar junction transistor

BJT can be used as an electronic switch to control brake lights though micro-controller. When the microcontroller outputs a “1” to pin D21 which means 5V output, brake lights on the kart is then turned on. On the other hand, the brake light is off if pin D21 has 0V output. BJT has two types, NPN transistors and PNP transistors. In this case, NPN type transistor is chosen because the working mechanism of NPN transistor can cope better with micro-controller. To elaborate on that, the NPN transistor is powered on when enough current is flowing through the base of the transistor. On the opposite, the base current in PNP transistor flows out by giving the lower base voltage than emitter voltage. Therefore, NPN type transistor is chosen because the microcontroller can easily supply a sufficient base current and power on the transistor.

	Requirement	2N3904TAR	2N6292
Transistor type	NPN/PNP	NPN	NPN
Rated voltage	12V	40V	70V
Price		£0.23	£0.73
Rated current	100mA	200mA	7A

Table 16. Comparisons between 2N3904TAR and 2N6292.

From Table 16, 2N39047TAR and 2N6292 both NPN transistors and satisfy the requirements of transistor. Theoretically, 2N3904TAR is the better choice as transistor because it provides all functions required and is cheaper but the transistor 2N6292 is used to test the brake light circuit because 2N6292 fits better on the stripboard than 2N3904TAR.

4.1.2. Brake lights circuit

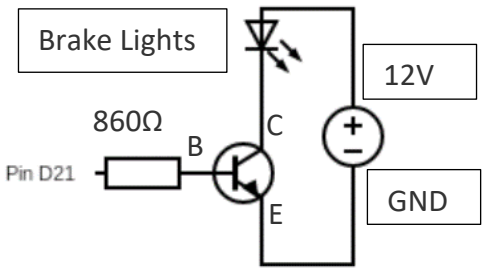

Figure 25. NPN transistor implementation of brake lights.

Figure 25 shows the circuit diagram of BJT controlled brake lights. Additionally, the brake light is turned on when pin D21 on the microcontroller is set to HIGH state, which outputs 5V. On the other hand, the brake light is turned off when pin D21 is set to LOW state.

Analysing this circuit, 12V supply in series with brake light, emitter and collector terminal of transistor. Most importantly, an 860Ω resistor is connected in series with pinD21 on the microcontroller to the base terminal of transistor to limit the base current flowing through the transistor and avoid overcurrent condition.

	DC current gain (min) (β)	Base-Emitter On voltage (max) $V_{BE(ON)}$	Collector current (I_C)	Base voltage (V_B)
Transistor 2N6292	30	3.0V	70mA	5.0V

Table 17. Characteristics of transistor 2N6292 and brake light circuit.

$$I_B = \frac{I_C}{\beta} = \frac{70mA}{30} = 2.\dot{3}mA \quad (10)$$

Since the minimum DC current gain of transistor 2N6292 is 30 from table 17, the biggest required base current ($2.\dot{3}mA$) to turn on the transistor and let collector current of 70mA flow through can be calculated from equation (10).

$$R_B = \frac{V_B - V_{BE}}{I_B} = \frac{5V - 3V}{2.\dot{3}mA} = 857\Omega \quad (11)$$

The resistance of base current limiting resistor can be calculated from equation (11) by ohm's law. To elaborate on that, the voltage across microcontroller (5V) and base terminal of powered on transistor (3V) is 2V. Moreover, a resistor is needed to restrain the base current under $2.\dot{3}mA$ provided this 2V voltage across.

4.1.3. CAN BUS communication

The brake signal is controlled by another Leonardo CAN BUS shield microcontroller at the front of the kart. To communicate with this Leonardo board, CAN BUS commination need to be established between two microcontrollers. The code of this CAN BUS communication is in Appendix 7.

Figure 26 shows the CAN BUS communication system of the brake signal. To be specific, once the brake is pressed, the microcontroller A will send out brake signal through CAN BUS. Furthermore, CAN_H and CAN_L pins on microcontroller A are connected to microcontroller B accordingly through D-sub connector.

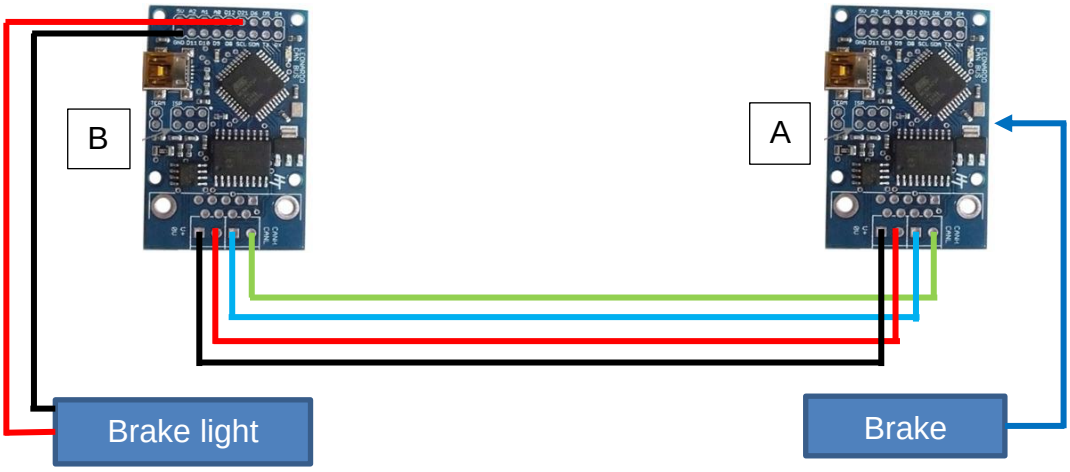

Figure 26. CAN BUS communication of brake signal.

```
------------------------------
Get data from ID: 20
0       0       1       0       0       0       0
------------------------------
Get data from ID: 20
0       0       0       0       0       0       0
```

Figure 27. CAN signal output on Serial monitor.

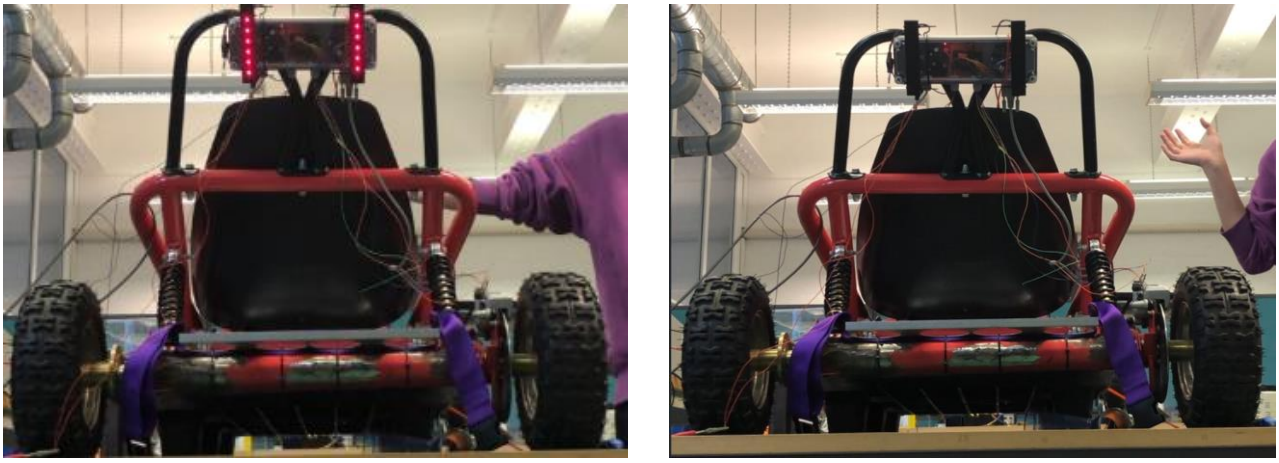

Figure 28. Brake light on (left) and off (right).

Figure 27 is the serial monitor output after filtering to be only print out signal transmitting using CAN ID 20. When the brake is pressed, the third bit of this array signal is configured to 1. On the other hand, the third bit of this array is configured to 0 when the brake is released.

Microcontroller B can use an if statement to check if the coming signal has CAN ID 20. If that is true, then turn on the brake light as in figure 28 (left) when the third bit is 1 or turn off the brake light as in figure 28 (right) when the third bit is 0.

4.2. Enclosure Design

Enclosure design is rather an essential procedure for this project because this RFID ignition system and brake light need to be compatible with the electric kart. Therefore, a carefully designed enclosure box is needed to contain all essential components, including buck converters, RFID readers, brake lights and Leonardo CAN BUS shield microcontroller. Furthermore, different power supply (48V, 12V and 5V) cables need to be connected between components inside enclosure box and devices on the kart. Additionally, a 9-pin d-sub connector is needed to enable the Leonardo CAN BUS shield to communicate with the micro-controller at the front of the kart.

4.2.1. Enclosure box selection

Since the enclosure box which fits requirements can be found in the online store, there is no reason to spend time to design and build an enclosure box for this project.

	Requirements
Enclosure height	>50mm
Enclosure length	>240mm
Enclosure width	>65mm
Lid type	Transparent lid
Material	Insulation material

Table 18. Requirements of the enclosure box.

From Table 18, there are some specific requirements of enclosure box used in this project. Firstly, dimensions of enclosure box need to be greater than the value specified in Table 18 in order to contain all devices. However, smaller enclosure boxes have more on-kart placing options. Secondly, lid of the enclosure box is better to be transparent. A transparent lid can present all devices contained in the enclosure box more clearly. Lastly, the enclosure box must be insulated. Conductive material may cause unwanted short circuits to some devices contained in the box.

	CHDX6-227C	CHDX6-228C	CHDX6-327C
Enclosure dimension (length × width × height in mm)	250 × 80 × 70	250 × 80 × 85	250 × 80 × 70
Material	Polycarbonate	Polycarbonate	ABS
Lid type	Transparent lid	Transparent lid	Transparent lid
Unit price	£8.99	£10.08	£10.25

Table 19. Properties of enclosure boxes.

CHDX6-227C is chosen as the enclosure box among all three choices shown in Table 19 for three

reasons. To begin with, CHDX6-227C and CHDX6-327C are smaller in size compared with CHDX6-228C because of 15mm less in height. Furthermore, CHDX6-227C and CHDX6-228C are both made of polycarbonate. On the other hand, CHDX6-327C is made of ABS. Polycarbonate is favoured because it is more durable compared with ABS. Lastly, CHDX6-227C is the cheapest among all three options.

4.2.2. Devices placing

Electronic devices including, two buck converters PCB, BJT control stripboard, double-LED control PCB, Leonardo CAN BUS shield microcontroller and RFID reader, need to be logically designed and placed into the enclosure box CHDX6-227C.

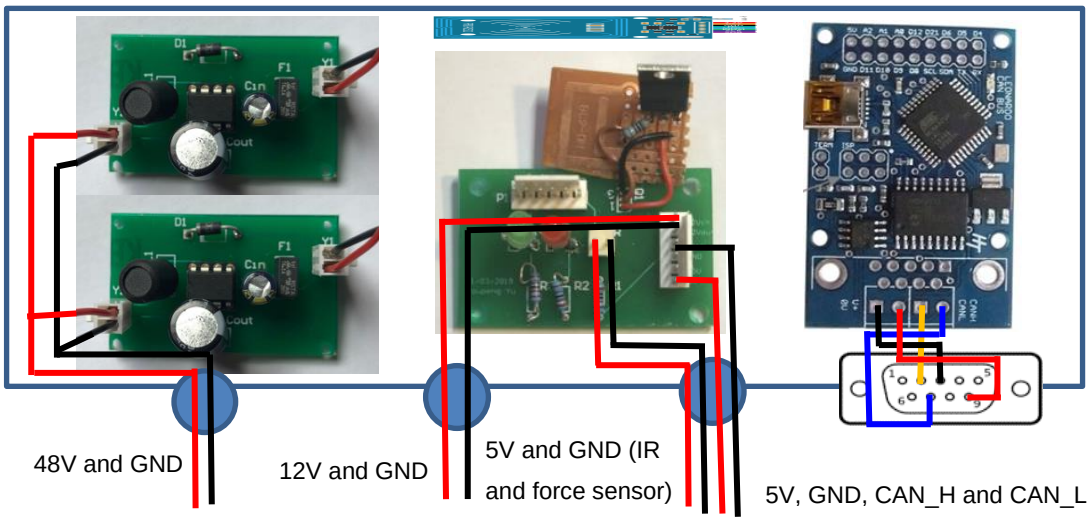

Figure 29. Plane view of the enclosure box.

From Figure 29, two buck converters (5V and 12V) are placed in parallel at the left hand of the enclosure box. From this placing, both buck converters can share the same input voltage cable of 48V which reduces the extra cable of 48V input. Double-LED control PCB is connected to BJT control stripboard as shown in Figure 29. Double-LED control PCB have two 6-pin Molex headers on board and that gives a neater connection of 12V supply for brake lights and 5V supply for both IR, force sensors. The RFID reader is placed vertically in parallel with the double-LED control PCB because this way it minimises the distance between RFID reader and box and guarantees RFID tags can be read once tapped on the top side of the box. Lastly, the Leonardo CAN BUS shield microcontroller is placed at the right side of this box because the double-LED control PCB must be placed at the middle of this box to avoid getting blocked by brake lights. To elaborate, two brake lights are placed at the left and right hand, and on top of the enclosure box. Therefore, to minimise the wiring trail and show the lightning status of LED, the microcontroller is placed at the right hand of the enclosure

box.

4.2.1. Cable glands and D-SUB connector

Holes to be drilled on the enclosure box to ensure cables go through boxes and make connections between devices inside and outside the box.

	ST PG7 cable glands	RS PRO M16 cable glands
Material	Polyamide	Nylon
Maximum cable diameter	6.5mm	7mm
Minimum cable diameter	2.5mm	3mm
Unit price	£0.944	£0.898

Table 20. Comparisons between two types of cable glands.

From Figure 30, three holes are drilled for cable glands represented by blue-filled circles and each hole has at least two wires going through and four at maximum. ST PG7 is chosen among these two options shown in Table 20 because it shrinks the minimum cable diameter to 2.5mm. With ST PG7 cable glands, 48V and 12V supply wires are safely constrained and not to be pulled out.

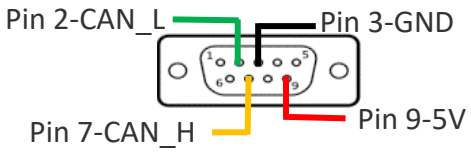

Figure 30. 9-pin d-sub connector layout.

Leonardo CAN BUS shield microcontroller can be used to receive and transmit CAN BUS signal and this unique feature is used to receive CAN BUS brake signal and control brake lights. Therefore, a 9-pin D-SUB male connector is mounted on the box as shown in Figure 30. There are 9 pins in D-SUB male connectors, 4 pins including CAN_H, CAN_L, 5V and GND are used for this CAN BUS communication. In this case, pin 2 and pin 7 are connected to the microcontroller to transmit CAN_L and CAN_H signals, respectively. Moreover, pin 3 and pin 9 are used to supply 5V to the microcontrollers at the front of the kart.

4.2.2. Brake light and enclosure box placing

From Figure 31, brake light is placed over the enclosure box and the enclosure box is placed at the back of the kart. By placing brake light over the enclosure box can shorten wires of connection for brake light. Furthermore, break light will be noticeable to pedestrians and cars behind when the kart's break is pressed.

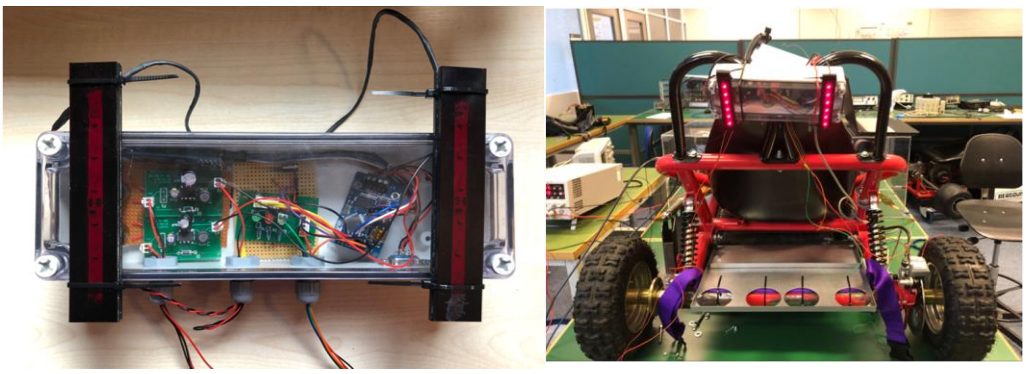

Figure 31. Brake light (left) and enclosure box (right) placing.

5. Conclusion and Future works

The 5 objectives of this project have all been achieved and implemented on the kart. To begin with, designing RFID ignition and self-locking system. A green LED is used to represent the locking state of the kart, and it can be turned on or off by tapping university student card. Furthermore, the green LED will be turned off automatically when both infrared sensors and force sensors cannot detect users are the seat for 15s. Secondly, two buck converter PCBs are used to provide 12V and 5V supply for brake lights and microcontrollers respectively. These buck converters can successfully step battery voltage of 48V down to 12V and 5V with rather high efficiency. In addition, fuses are implemented for buck converter PCBs to protect essential components and fuses can be easily replaced by unscrewing fuse holders. Thirdly, CAN BUS communication between the microcontroller at the front of the kart and Leonardo CAN BUS shield microcontroller are successfully implemented through the D-sub connector. Through CAN BUS communication, Leonardo board can receive brake signal and turn on or off the brake light through BJT control. Lastly, an enclosure box with cable glands and a d-sub connector is used to contain all electronic devices. Furthermore, the brake light is fixed on the enclosure box and then together placed at the top back of the kart to make the brake light more noticeable for pedestrians and cars behind.

There are some further improvements that can be done to the self-locking system in this project. The self-locking system is aimed to self-lock the kart when users are not around for a period of time, and the user detection system becomes rather important for accurately reflect the seat status. However, the user detection system used in this project cannot distinguish between an object and a user. This can be improved by adding a variation range to arithmetic of force sensors or importing other types of sensors. This RFID ignition system is not technically a “keyless” ignition system, because this system still requires RFID cards, such as university student cards to be brought with users. The keyless ignition system would be looking into unlock with biological evidence. To be specific, fingerprint lock, facial recognition and iris-bases identity authentication are good choices as biometrical locks on kart.

6. References

[1] Assets.publishing.service.gov.uk. (2017). [online] Available at: https://assets.publishing.service.gov.uk/government/uploads/system/uploads/attachment_data/file/776083/2017_Final_emissions_statistics_one_page_summary.pdf [Accessed 4 Apr. 2019].

[2] Home, Transport and vehicles, E. (2019). Electric vehicles. [online] Energy Saving Trust. Available at: https://www.energysavingtrust.org.uk/transport/electric-vehicles [Accessed 4 Apr. 2019].

[3] Boeriu, H. (2018). BMW introduces the Key fob with touchscreen display. [online] BMW BLOG. Available at: https://www.bmwblog.com/2015/01/06/bmw-introduces-key-fob-touchscreen-display/ [Accessed 15 Nov. 2018].

[4] Lichtermann, J., Pettit, R. "Automotive Application of Biometric Systems and Fingerprint," SAE World Congress, March 2000.

[5] Juels, A. (2006). RFID security and privacy: a research survey. IEEE Journal on Selected Areas in Communications, 24(2), p.3. C. Security and Privacy Problems.

[6] Trossenrobotics.com. (n.d.). [online] Available at: http://www.trossenrobotics.com/productdocs/2010-10-26-datasheet-fsr402-layout2.pdf [Accessed 4 Apr. 2019].

[7] Lecture notes for EEEN30042 Power Electronics. (2018). University of Manchester.

[8] http://www.ti.com/lit/ds/symlink/lm2574hv.pdf. (2018). LM2574x SIMPLE SWITCHER® 0.5-A Step-Down Voltage Regulator. [online] Available at: http://www.ti.com/lit/ds/symlink/lm2574hv.pdf [Accessed 5 Apr. 2019].

7. Appendices

7.1. Appendix 1 Arduino library code of function `MFRC522::PICC_IsNewCardPresent()`

```
bool
MFRC522::PICC_IsNewCardPresent()
{
                                        byte bufferATQA[2];
                                        byte bufferSize = sizeof(bufferATQA);

                                        // Reset baud rates
                                        PCD_WriteRegister(TxModeReg, 0x00);
                                        PCD_WriteRegister(RxModeReg, 0x00);
                                        // Reset ModWidthReg
                                        PCD_WriteRegister(ModWidthReg, 0x26);

                                        MFRC522::StatusCode result =
                                    PICC_RequestA(bufferATQA, &bufferSize);
                                        return (result == STATUS_OK || result ==
                                    STATUS_COLLISION);
                                    } // End PICC_IsNewCardPresent()
```

7.2. Appendix 2 Arduino code of function `IsNewCardCorrect()`

```
bool IsNewCardCorrect() {

  if ( ! mfrc522.PICC_IsNewCardPresent()) {
  return false;
  }

  // Select one of the cards
  if ( ! mfrc522.PICC_ReadCardSerial()) {
  return false;
  }

  Serial.print("UID tag :");
  String content= "";
  byte letter;
  for (byte i = 0; i < mfrc522.uid.size; i++)
  {
     Serial.print(mfrc522.uid.uidByte[i] < 0x10 ? " 0" : " ");
     Serial.print(mfrc522.uid.uidByte[i], HEX);
     content.concat(String(mfrc522.uid.uidByte[i] < 0x10 ? " 0" : " "));
     content.concat(String(mfrc522.uid.uidByte[i], HEX));
  }

  Serial.println();
  content.toUpperCase();
```

```
  if (content.substring(1) == "04 5D 53 6A 5E 43 80")
  {
    Serial.println("Message : Authorized Acess");
    delay(2000);
    Serial.println();
    return true;
  }
  else {
    Serial.println("Message : No Acess");
    delay(2000);
    Serial.println();
    return false;
  }
}
```

7.3. Appendix 3 main loop of unlock and lock the kart and functions

```
void loop() {
//  Serial.print(r);
//
//  Serial.print("  ");
//
//  Serial.println(digitalRead(LED_G));


  if (r==1){
    if (IsNewCardCorrect()){
      Unlock();
      r=0;
    }
    else{
      return;
    }
  }
  else{
    if (IsNewCardCorrect()){
      Lock();
      r=1;
    }
    else{
      return;
    }
  }

  //Serial.println(IsNewCardCorrect());

}
```

```
  void Lock(){
    digitalWrite(LED_G, LOW);
    delay(2000);
  }
  void Unlock(){
    digitalWrite(LED_G, HIGH);
    delay(2000);
  }
```

7.4. Appendix 4 main loop of user detection system

```
void loop(){
  Serial.print(Detection())
  Serial.println(digitalRead(LED_G));

  if(Detection() == false){
    for(int i=0; i<20; i++){
      if(Detection() == true){
        return;
      }
      else {
          Serial.println(digitalRead(LED_G));
          delay(500);
      }
    }
    if(Detection() == false){
      digitalWrite(LED_G, LOW);
    }
    else {
      return;
    }
  }
  else {
    return;
  }
}


bool Detection(){
     force = analogRead(pressurePin);
     isObstacle = digitalRead(isObstaclePin);
     if (force > 500 || isObstacle == LOW) return true;
     else return false;
 }
bool ForceResult(){

  force = analogRead(pressurePin);
  if (force>500)return false;
```

```
  else return true;
}
```

7.5. Appendix 5 table of FSR resistance against force

	Force in Nm	Resistance in ohms
No mass	0	Infinite
20g mass	0.2	30k
50g mass	0.5	10k
100g mass	1	6k
230g mass	2.3	3.1k
500g mass	5	1.8k
1000g mass	10	1k
2000g mass	20	700
4000g mass	40	450
7000g mass	70	300
10000g mass	100	250

7.6. Appendix 6 pin layout of FC-51 IR proximity sensors and Leonardo CAN BUS shield

	FC-51 IR proximity sensors	Leonardo CAN BUS shield
Power	Pin Vcc	5V
GND	Pin GND	GND
Signal output from sensor	Pin Out	D5

7.7. Appendix 7 CAN BUS communication code

```
const int SPI_CS_PIN = 17;

MCP_CAN CAN(SPI_CS_PIN);                                    // Set CS pin

void setup()
{
    Serial.begin(115200);
    pinMode(Control, OUTPUT);
    pinMode(Ground, OUTPUT);
    digitalWrite(Ground,LOW);

    while (CAN_OK != CAN.begin(CAN_100KBPS))              // init can bus : baudrate = 500k
    {
        delay(100);
```

```
    }
}


void loop()
{
    unsigned char len = 0;
    unsigned char buf[8];

    if(CAN_MSGAVAIL == CAN.checkReceive())            // check if data coming
    {
        CAN.readMsgBuf(&len, buf);    // read data,  len: data length, buf: data buf

        unsigned int canId = CAN.getCanId();
        if(canId == 20 && buf[2]==1){
            digitalWrite(Control,HIGH);
        }
        else if(canId == 20 && buf[2]==0){
        digitalWrite(Control,LOW);
        }
    }
}
```